

Because phonons interact with electronic states via electric fields,²⁶ there can be no first-order direct phonon relaxation between the components of a Kramers doublet. If such Kramers doublets could be split with far i.r. separations (either by external magnetic fields or internal exchange fields) then magnetic dipole electronic transitions would be allowed but phonon transitions could be weak.

Impurity-doped crystals have proven to be good laser materials for wavelengths longer and shorter than far

i.r. wavelengths. It is possible that doped crystals can be found to serve as laser materials for far i.r. wavelengths also. The investigation of such possibilities as indicated above and other special situations should give interesting results.

ACKNOWLEDGMENTS

We are grateful to Dr. R. M. Macfarlane and Professor P. L. Scott for a number of helpful discussions.

Mode Interaction in a Zeeman Laser*

W. CULSHAW AND J. KANNELAUD

Lockheed Palo Alto Research Laboratory, Palo Alto, California

(Received 2 November 1966)

The interaction between modes of a short He-Xe laser using the $J=1 \rightarrow 0$ transition at 2.65μ is investigated in an axial magnetic field. In zero field an elliptically polarized output usually predominates, with orientation and eccentricity changing with conditions and reflector characteristics. Neutral coupling occurs here; consequently, the system is sensitive to perturbations, in agreement with the observed erratic behavior. Small axial magnetic fields produce circular polarizations, quenching, and hysteresis effects between the two Zeeman oscillations arising from the frequency splitting of a single axial mode. A strong interaction, including sharp crossover regions in the intensities and quenching phenomena, is observed between two axial modes oscillating on well-resolved oppositely circularly polarized Zeeman components. The phenomena are studied as a function of cavity tuning, laser intensity, pressure, and magnetic field. No hysteresis was observed in the interaction between axial modes. The axial-mode intensities are equal for all positions of cavity tuning when the Zeeman separation equals the axial-mode interval. For small deviations of magnetic field from this value, however, crossover and quenching effects appear, and this allows a precise determination of the g value of the upper state. These effects are discussed on the basis of Lamb's theory and equations deduced for the interaction. The Doppler parameter Ku is about 100 Mc/sec for xenon, which is comparable with the natural linewidths, and requires a more exact discussion of the third-order atomic polarization terms. The results derived show some qualitative agreement with observations, particularly on the axial-mode interaction, which is discussed in detail.

I. INTRODUCTION

IN this paper we shall be concerned with the effects of axial magnetic fields on a short He-Xe laser operating on a $J=1 \rightarrow 0$ transition at 2.65μ . Previous work¹ on the He-Ne, $J=1 \rightarrow 2$ laser transition at 1.153μ has shown that the polarization of an internal-mirror, or planar-type, laser is linear in zero magnetic field. Also, in near-zero axial magnetic fields, a rotation of this linear polarization occurs up to a maximum of $\pm \frac{1}{4}\pi$, and is a result of a mutual locking of the circularly polarized oscillations due to the proximity of their frequencies. With increasing magnetic field, both circularly polarized oscillations occur simultaneously, and low-frequency beats appear as a result of the frequency splitting of the single axial mode involved.

The results obtained with an axial magnetic field on the He-Xe laser are entirely different in most respects.

The occurrence of low-frequency beats seems to be much less pronounced and has not been observed so far. In zero magnetic field, the polarization tends to be circular or elliptical, and only in rare instances in a linear polarization observed at low intensities. Rotations of the elliptic polarization with cavity tuning and magnetic field have been observed at times, but such results are erratic and not reproducible. They are highly dependent on the past history of the system, such as reflector changes, intensity of oscillation and direction of cavity tuning, and on the gas pressure.

The results obtained on the He-Ne transition in near-zero magnetic fields substantiate the result deduced by Heer and Graft² that in a $J=1 \rightarrow 2$ transition the singular point representing simultaneous oscillations on both circular polarizations is stable. This result is derived for the laser tuned to the line center, and for perfectly isotropic reflectors. The presence of a small anisotropy in the reflectors, and the near coinci-

* Supported by the Lockheed Independent Research Funds.

¹ W. Culshaw and J. Kannelaud, *Phys. Rev.* **136**, A1209 (1964); **141**, 228 (1966); **141**, 237 (1966).

² C. V. Heer and R. D. Graft, *Phys. Rev.* **140**, A1088 (1965).

dence of the frequencies of these oscillations, lead to a mutual synchronization of them, and hence to a polarization that is linear in zero field and that rotates as an axial magnetic field is applied.² A similar conclusion that the polarization of a $j \rightarrow j \pm 1$ ($j \neq 0$) transition should be linear in zero magnetic field has been given by Doyle and White,³ who have analyzed a general laser transition involving degenerate atomic states. Some results of a similar nature have also been given by Polder and Haeringen.⁴

In view of the above stability for simultaneous circularly polarized oscillations in the He-Ne, $J=1 \rightarrow 2$ laser transition, the results in near-zero magnetic fields were much more reproducible than those obtained here on the $J=1 \rightarrow 0$ transition of the He-Xe laser. For this transition, Heer and Graft² indicate that the singular point of the nonlinear equations representing simultaneous oscillations on both circularly polarized components tends to be a saddle point—this again for near-zero magnetic field, perfect mirrors, and the cavity tuned to line center. This conclusion is also reached in the present work, where it is shown that for similar conditions the coefficients β and θ , in the usual terminology for the nonlinear equations, become equal. Hence $\beta_1\beta_2 = \theta_{12}\theta_{21}$, a condition which is sometimes designated as neutral coupling. Such a system is likely to be quite sensitive to the past history and operating conditions of the laser, in agreement with the erratic behavior encountered in the present investigations in zero magnetic field.

The application of small axial magnetic fields to the He-Xe laser made the observations somewhat more reproducible. Here, in addition to possible stable operation on the two oppositely circularly polarized modes giving a crossover region in the intensities as the cavity is tuned through the center of the line, it is possible for a stable situation to occur in which one mode quenches the other, the particular mode of operation, or polarization, depending on the directions of cavity tuning and magnetic field. Hysteresis effects also occur, the favored oscillation persisting until the cavity has tuned through line center by an amount depending on the magnetic field. The opposite polarization behaves in a similar way as the cavity is scanned in the opposite direction, leading to a bistable region of operation near line center.⁵ Similar observations on the He-Ne 1.52- μ $J=1 \rightarrow 0$ transition have been made by Fork *et al.*,⁶ and also by Lang and Bouwhuis.⁷ The conditions for simultaneous oscillations or crossover regions in the neighborhood of the line center, while still apparently sensitive to conditions, seem more readily attainable on

this transition than in our experiments on the Xe transition. This is possibly due to the smaller value of the Doppler parameter $Ku \sim 100$ Mc/sec than the value of some 380 Mc/sec for the Ne transition. An atomic temperature of some 500°K is assumed in these values.

An interesting, and potentially useful, result of our investigations is that a strong interaction is also observed between axial modes of a short Xe laser operating on well-resolved Zeeman components in an axial magnetic field. This is particularly so when the Zeeman splitting of the $m = \pm 1$ sublevels approaches the frequency separation between two axial modes of the cavity. For values of magnetic field slightly higher than that equivalent to this frequency separation, the circularly polarized $\Delta m = -1$ oscillation quenches the $\Delta m = \pm 1$ oscillation as the cavity is tuned to higher frequencies across the Doppler linewidths of these transitions. Near the symmetrical position of the cavity modes with respect to these Zeeman components a crossover region occurs, and the intensities of the two simultaneous oscillations become equal at the symmetrical position. On tuning towards higher frequencies beyond this point, the $\Delta m = +1$ oscillation quenches the $\Delta m = -1$ oscillation. The situation is the opposite of this for values of magnetic field slightly less than that equivalent to the axial-mode separation. When the Zeeman separation of the $\Delta m = \pm 1$ transitions is exactly equal to the axial-mode separation of the cavity, the intensities of the two oscillations are equal for all positions of cavity tuning. Such results were quite reproducible, in contrast to the observations on a single axial mode in near-zero magnetic fields. The sharp crossover regions may be used for frequency stabilization of the laser, whereby two axial modes of the laser are frequency stabilized by the atomic transition at offset frequencies determined by the cavity length and mode numbers. The value of magnetic field at which the intensities of the two oscillations remain equal for all cavity tuning positions may be used to determine the g value of the transition, and such a method is found to be quite precise.

The nonlinear interaction between axial modes operating on well-resolved circularly polarized Zeeman components theoretically is expected to be somewhat smaller than the interaction between such oscillations arising from a single axial mode in near-zero magnetic fields. One of the main aims of the present work is thus concerned with the explanation of the observed strong interactions, including the quenching of one axial mode by the other. Here the smaller value of Ku for the Xe transition is found to be particularly significant, and the delta-function approximation used initially by Lamb⁸ in the evaluation of the third-order contribution to the atomic polarization is no longer satisfactory. Such integrals must be evaluated exactly. Collision effects are also significant, and may be con-

³ W. M. Doyle and M. B. White, *Phys. Rev.* **147**, 359 (1966).

⁴ D. Polder and W. Van Haeringen, *Phys. Letters* **19**, 380 (1965).

⁵ J. Kannelaud and W. Culshaw, *Appl. Phys. Letters* **9**, 120 (1966).

⁶ R. L. Fork, W. J. Tomlinson, and L. J. Heilos, *Appl. Phys. Letters* **8**, 162 (1966).

⁷ H. DeLang and G. Bouwhuis, *Phys. Letters* **20**, 383 (1966).

⁸ W. E. Lamb, Jr., *Phys. Rev.* **134**, A1429 (1964).

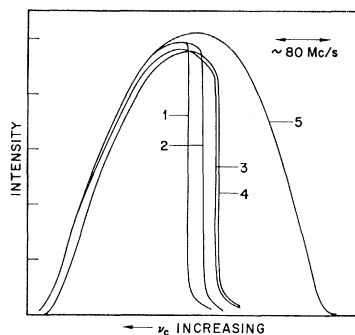


FIG. 1. Intensity of right-handed circularly polarized Zeeman component versus cavity tuning for small values of magnetic field ($m=1 \rightarrow 0$ transition). Vertical lines show tuning positions at which polarization abruptly changes to left circular. Curve No. 1, $H=5.35$ G; curve No. 2, 2.14 G; curve No. 3, 1.07 G; curve No. 4, 0.107–0.54 G. No. 5 shows the total output in both modes. Cavity scan from left to right. Relative laser intensity +4 dB.

sidered to some extent by using the hard and soft collision processes introduced by Szöke and Javan,⁹ and modifying the atomic response to the radiation wherever it occurs in the formula for the Zeeman laser. We proceed by giving first the experimental results obtained on the mode interaction in a short He-Xe laser operating at 2.65μ on the $J=1 \rightarrow 0$ transition. These somewhat unexpected results, particularly the strong axial-mode interaction, must then be explained by the theory which follows.

II. EXPERIMENTAL

The following represents some of the results obtained on a He-Xe laser operating at 2.65μ on the $5d[\frac{3}{2}]_1^0 - 6p[\frac{1}{2}]_0$ transition of Xe.¹⁰ Specifically, results are given on the polarization and other characteristics of the oscillations in zero magnetic field and at small axial magnetic fields of a few gauss, together with similar nonlinear phenomena which occur when the magnetic field is near the value which produces a Zeeman separation corresponding to the axial-mode frequency separation of the laser. The results were obtained using a planar-type internal-optics laser, with a dc discharge 3 mm in diam and 10-cm long. The reflector spacing was 20.65 cm, giving an axial-mode frequency interval of 726 Mc/sec. Axial magnetic fields were applied with a solenoid 3.2 cm in diam and 14.5 cm in length which produced a magnetic field of 53.5 G/A. The field was quite uniform over the central 6-cm portion of the solenoid and varied by 1% over a total length of 8 cm, and up to 2% over the total 10-cm length of the discharge. The solenoid and the discharge were enclosed in a magnetic shielding box of Mumetal, and electrostrictive ceramic tuning of the laser was provided. Most of the experiments used pressures of 2.8 Torr He and 0.1 Torr Xe, but there was no change in the main

⁹ A. Szöke and A. Javan, Phys. Rev. Letters **10**, 521 (1963); Phys. Rev. **145**, 137 (1966).

¹⁰ W. L. Faust, R. A. McFarlane, C. K. N. Patel, and C. G. B. Garrett, Appl. Phys. Letters **1**, 85 (1962).

features of the axial mode interaction at other pressures. Isotopically enriched Xe was used with 84% Xe¹³⁶ and 14% Xe¹³⁴ as major constituents.

A. Near-Zero Magnetic Fields

As already noted, the polarization of this laser in zero field is completely different from the linear polarization observed with the He-Ne $1.153\text{-}\mu$ laser transition. Initially, at high oscillation intensities a right-handed circularly polarized output was observed in zero magnetic field. This corresponded to the polarization observed when a magnetic field, directed away from the observer, was applied to the laser, indicating that this sense of polarization corresponded to the high-frequency Zeeman component. On reversing the field and increasing it to about 2 G, the polarization abruptly reversed to left circular. The right-handed circular polarization in zero magnetic field was observed for all positions of cavity tuning. However, on tuning the laser to the low-frequency side of the Doppler line-width, a magnetic field of the opposite direction to that used before was required to reverse the polarization from right- to left-handed circular. When the oscillation intensity was decreased, the output became elliptical in zero magnetic field, and at very low intensities it became linearly polarized.

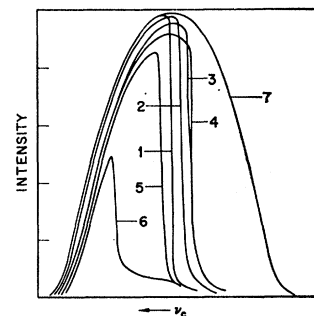
After some minor modifications to the apparatus, which required a partial disassembly of the laser and opening of the vacuum envelope, the circular polarization in zero magnetic field was no longer observed. Instead, the output became elliptically polarized, with the ratio of major to minor axes increasing as the oscillation intensity was decreased. The sense of the polarization was again right handed, and the application of a magnetic field, besides rendering the output circularly polarized, affected the sense of polarization in the manner described above. At other times, after further modifications and possible changes in the reflectors, the output in zero field was circularly polarized and remained circular at relatively low powers, in contrast to previous results. It is obvious that the polarization characteristics in zero magnetic field are highly dependent on the past history of the laser.

Attempts were made to determine whether the direction of the major axis of the ellipse (or, at low intensities, the linear polarization) rotates with cavity tuning and with small applied magnetic fields. The results were somewhat inconclusive because they were erratic and not reproducible. In zero magnetic field, rotations of the ellipse of up to 60° have been observed at times when the cavity was detuned to either side of line center. Such results were not, however, reproducible, and sometimes under apparently identical conditions no rotation at all was observed. The direction of rotation was the same regardless of cavity tuning, and when it did occur, it was more predominant at high oscillation intensities.

Similar erratic behavior was observed in the rotation of the ellipse with small magnetic fields. In this case, however, the rotation was much less, usually no more than 15° , and only on rare occasions was a rotation as large as 30° observed. The same results were obtained whether the cavity was tuned to line center or off line center. The polarization changed from elliptical or linear to circular as the field increased to some 2 G, but this change was not always monotonic. After the circular polarization was attained in an axial magnetic field, the observations became more consistent. Figure 1 shows the variation in the intensity of the right-handed circularly polarized oscillation as the cavity is scanned from left to right for various small values of magnetic field. The abrupt decrease in the intensity shows the tuning position at which the polarization of the oscillation abruptly changes to left circular. It is seen that such positions extend beyond the line center as fixed by curve 5, which is the sum of both polarizations. If the cavity is tuned into the line from right to left, a similar hysteresis effect is observed in the left-hand circularly polarized oscillation. The position of the jump clearly depends on the applied magnetic field, and gives rise to a bistable region of oscillation. A similar effect is also found in the He-Ne $1.52\text{-}\mu$ $J=1 \rightarrow 0$ transition.⁶ It appears from Fig. 1 that the width of the bistable region is greater at the smaller values of magnetic field used here. Figure 2 shows similar results taken at a lower level of laser intensity, and also with one of the reflectors rotated by 90° . The results are quite similar and indicate that the phenomenon is fairly reproducible. The general trend of both sets of curves from 5.35 to 0.53 G is the same. Figure 2 shows a deviation from the trend at the lower values of 0.267–0.107 G, which is possibly due to variations in the polarization as discussed above at these smaller values of magnetic field and laser intensity. The curves substantiate the result mentioned earlier that the polarization may be switched from right to left circular by a magnetic field applied in the appropriate direction.

In past investigations we have found that small anisotropies in the reflectors used in the laser cavity can have a profound effect on the operation, and especially on the polarization characteristics of the laser. Such appears to be the case here, particularly in zero magnetic field, as changes occurred when one of the reflectors was rotated by 90° . The output power decreased by a few dB, the polarization was again elliptical in zero magnetic field, but the major axis had rotated to a new direction. The sense of the polarization was the same as before (right handed). Considerable hysteresis effects were, however, noted in this case. For example, frequency when the laser was operated in zero field and the polarization characteristics observed, and then a magnetic field applied and returned to zero, the polarization had rotated to a different direction, and the degree of ellipticity had changed. The original mode of oscilla-

FIG. 2. The same as in Fig. 1, but with lower relative laser intensity of 0 dB. Curve No. 1, 5.35 G; curve No. 2, 2.14 G; curve No. 3, 1.07 G; curve No. 4, 0.54 G; curve No. 5, 0.27 G; No. 6, 0.11 G; curve No. 7 shows the total output in both polarizations.



tion could be obtained only by stopping and restarting the oscillation.

B. Axial-Mode Interaction

In order to avoid additional nonlinear complications, such as frequency locking effects due to the close proximity of the mode frequencies in near-zero fields, the output of the $2.65\text{-}\mu$ He-Ne laser was next studied when the magnetic field was sufficiently large as to allow simultaneous oscillations on well-resolved Zeeman components by two adjacent axial modes of the laser cavity. Of particular interest was the case where the Zeeman splitting of the $m = \pm 1$ sublevels was equal to or near the frequency separation (726 Mc/sec) of the axial modes of the cavity. The two oscillations of orthogonal circular polarizations were then studied as a function of cavity tuning, magnetic field strength, pressure, and oscillation intensity. A strong interaction between these Zeeman oscillations was found, even when they were separated well beyond their Doppler widths. This was evidenced by the regions of cavity tuning in which one mode quenched the other. Only when the magnetic field separation was equal to the axial-mode separation did both modes oscillate simultaneously and with equal intensities for all cavity-tuning positions. At other neighboring values of magnetic field, both modes oscillated simultaneously when the cavity tuning was near the symmetrical position with respect to the Zeeman components. At the exact symmetrical position, a sharp crossover region in the intensities occurred.

Some further differences in the operation of this laser as compared with previous observations on He-Ne lasers should first be noted. Figure 3 shows the laser output as a function of cavity tuning. It is apparent from the curve for zero magnetic field that no Lamb dip occurs. Under no operating conditions was any dip observed, although the intensity and pressure were varied over a wide range. Another effect is the tail seen in the low-frequency end of the plot of output versus cavity tuning in Fig. 3, which extends to some 350 Mc/sec from the line center. This was more predominant at lower pressures and is probably associated with the 14% isotopic content of Xe.¹³⁴ Such a mixture of isotopes would also affect the dip phenomena, but this may not be the reason for its absence under any operating conditions.

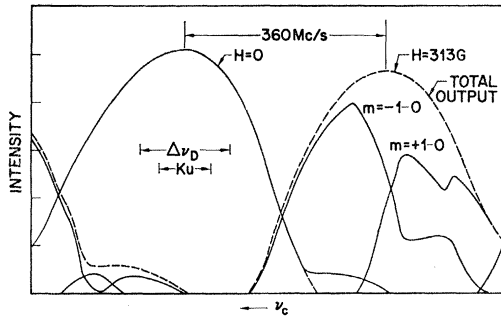


FIG. 3. Laser output versus cavity tuning for zero magnetic field and an axial field of 313 G. Relative laser intensity +8.5 dB. $\Delta\nu_D$ is the Doppler width.

Another observation from Fig. 3 (zero magnetic field) is that oscillations persist for large cavity detunings even on the high-frequency side where no tail exists. The threshold range of tuning depends on the excitation parameter η , but the range of some $3Ku$ seems large unless the natural linewidth, or the effective atomic response, is becoming comparable with Ku .

On applying an axial magnetic field to the laser, both left- and right-handed circularly polarized oscillations in two adjacent axial modes are seen in the output. Figure 3 also shows (dashed curve) the total output when a magnetic field approximately equal to the axial-mode spacing of the cavity is applied, together with the curves for the two circular polarizations. These were obtained by passing the laser output through a quarter-wave plate followed by an analyzer, and were taken at a relatively high level (8.5 dB relative) of laser intensity. The two circularly polarized outputs from the adjacent axial modes show the quenching phenomena. It is seen that over a large range of cavity tuning only one

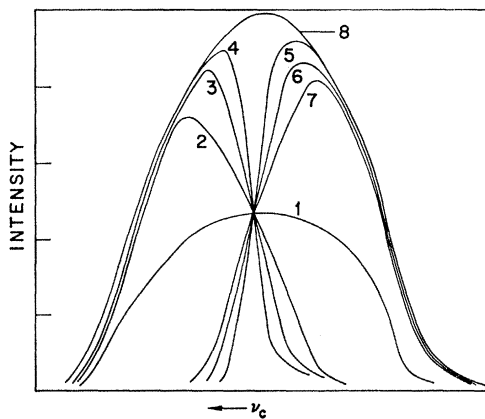


FIG. 4. Interaction between two axial modes of the laser acting on well-resolved Zeeman components versus cavity tuning. Curve No. 1, $H=316$ G, intensities of both circular polarizations equal for all tuning positions. Curves No. 2 through 7 for values of H equal to 313, 310, 305, 327, 322, and 319 G, respectively, shown for the left-handed $m=-1 \rightarrow 0$ transition. Right-handed $m=+1 \rightarrow 0$ transition opposite of these curves. Curve No. 8 shows the total output in both polarizations. Relative laser intensity 3 dB. Note crossover and quenching regions. Cavity scan from left to right.

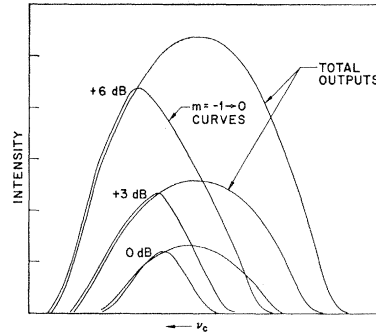


FIG. 5. Ratio of width for two simultaneous modes of oscillation to total width of oscillation (R) versus laser intensity. Relative intensity 0 dB, $R=0.24$; +3 dB, $R=0.30$; +6 dB, $R=0.46$. Axial magnetic field 310 G. Left-handed $m=-1 \rightarrow 0$ transition.

of the two modes oscillates, indicating a strong interaction between the two adjacent axial modes. This quenching phenomenon is critically dependent on the magnetic field strength in the region where this is close to the axial-mode separation of the cavity. Figure 4, which was taken at some 5 dB lower intensity (3 dB relative), shows the intensity of the left-handed circular polarized mode ($\Delta m=+1$ transition) as the magnetic field is varied by small amounts. It is seen that at this lower value of intensity the curves are more symmetrical, and the tail effect discussed above is not so pronounced. The curves for the right-handed circularly polarized oscillation ($\Delta m=-1$ transition) are essentially given by the mirror image of the appropriate curve in the vertical axis of symmetry. For a value of magnetic field apparently equal to the axial-mode spacing (316 G) both left- and right-handed circularly polarized modes oscillate simultaneously for all positions of cavity tuning (no quenching), and furthermore have the same intensity. However, when the magnetic field deviates by a fraction of 1% from this value, the quenching phenomenon appears. This suggests an accurate and sensitive method of determining the g values of atomic levels that have suitable J values and laser transitions. Using the value $\nu_L=1.40 \times H$ Mc/sec (H in G) for the Larmor frequency, with the axial-mode interval 726 Mc/sec and $H=2 \times 316$ G, we find a g value of 0.82 ± 0.01 for the $5d[\frac{3}{2}]_1^0$ state of Xe. The precision of the method is much higher, but non-uniformity and errors in the magnetic field limit the accuracy at present. However, the result does agree with a previous value of 0.82 ± 0.03 deduced for this level by a completely independent method.¹¹

All the curves in Fig. 4 display the left-handed circularly polarized mode. The opposite polarization would be displayed by rotating the analyzer by 90° . We note that as the cavity resonance frequency is swept from higher to lower frequencies (left to right in Fig. 4), for the magnetic fields below the value for axial-mode Zeeman separation, the left-handed polarization, corresponding to the low-frequency Zeeman component in our experiments (magnetic field directed away from observer), breaks into oscillation first; whereas for

¹¹ R. L. Fork and C. K. N. Patel, Appl. Phys. Letters 2, 180 (1963).

magnetic fields higher than this value, the right-handed polarization, corresponding to the high-frequency Zeeman component, oscillates first. The same phenomena were observed at all levels of laser intensity. Figure 5 shows a comparison of the effect at several levels of intensity. It is apparent that the quenching phenomenon becomes more predominant at lower intensities, i.e., the ratio of the range of cavity tuning where two modes can oscillate to the total width of oscillation decreases. The shape of the power-output curves of the two modes may at times depend fairly critically on factors not studied in detail at this time. Nearly all our observations yielded curves similar to those shown in Figs. 3 to 5; but in some isolated instances more complicated shapes were apparent, although the general features of the strong interaction were still present. Such differences would seem due to minor mechanical changes in the alignment of the laser. However, in general, our results have been quite reproducible.

Although the interaction between the two modes is quite sensitive to the value of magnetic field when this is close to the axial-mode frequency interval, the quenching effect has also been observed at values of magnetic field which differ by as much as 150 G from this particular value. Such a case is shown in Fig. 6 for a magnetic field of 423 G, at which the Zeeman splitting is much greater than the axial-mode separation of the laser, but quite a definite quenching is seen at the respective extremes of the output curves for both circular polarizations.

The mode competition and quenching effect may also be studied by keeping the cavity tuning fixed and sweeping the magnetic field. This was, however, experimentally more difficult. Figure 7 shows the intensity of the right-handed circularly polarized mode versus magnetic field for several cavity tunings near the symmetrical position. The symmetrical curve corresponds to a symmetrical tuning of the axial modes of the cavity with respect to the Zeeman components, and again quenching is observed when the cavity is detuned from this frequency.

An attempt was made to determine the effects of the total pressure on the above phenomena in order to see

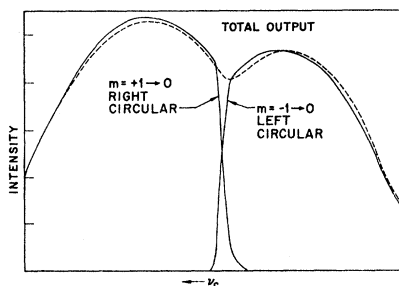


FIG. 6. Quenching phenomena between axial modes for the case where Zeeman separation is very different from the axial-mode frequency interval. Axial magnetic field 423 G (compare 316-G axial-mode interval). Relative laser intensity +7 dB.

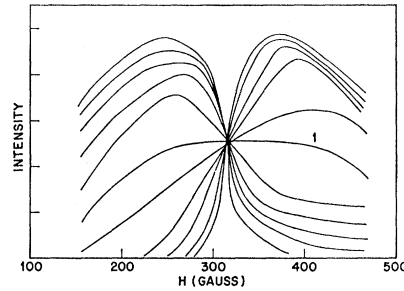


FIG. 7. Intensity of right-handed $m = +1 \rightarrow 0$ axial mode versus axial magnetic field for various cavity tuning positions. Curves taken at cavity tuning intervals of 15 Mc/sec increasing upwards. Curve No. 1, laser tuning symmetrical with respect to the Zeeman components. Relative laser intensity +7 dB.

their dependence on collision processes. For this the ratio of the partial pressures of helium and xenon was kept constant, but the total pressure was varied between 0.9 and 6 Torr. Results showed that the quenching phenomena are unaffected by pressure variations, but the line shape seems strongly dependent on pressure. Specifically, the anomalous tail in the line shape, mentioned previously as probably due to the isotope Xe^{134} , becomes much more predominant at low pressures and disappears completely at high pressures. Figure 8 shows typical results for the interaction in the low-pressure region. It is as though two atomic responses were now effective, with two crossover regions occurring as the cavity tuning is scanned over the composite line.

III. INTERPRETATION OF RESULTS

The observations which the theory must explain have been detailed in Sec. II. In particular, they are the strong quenching and hysteresis effects in near-zero magnetic fields and the erratic behavior of the polarization of the emission in zero magnetic field, which is dependent on the reflector characteristics, intensity, and tuning of the laser. Also needing explanation is the very strong interaction between axial modes of the laser (726 Mc/sec apart) operating on well-resolved Zeeman components whose separation is near this axial-mode interval of the laser. The sharp dependence of the quenching phenomenon on the magnetic field in

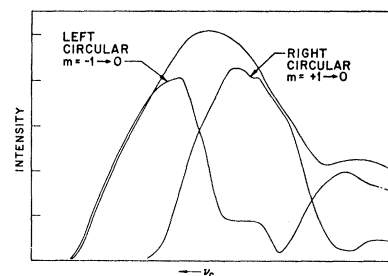


FIG. 8. Axial-mode intensities versus cavity tuning for total gas pressure of 0.9 Torr. (Curves should be compared with those in Fig. 4 taken at 2.9 Torr total pressure). Axial magnetic field 310 G. Relative laser intensity +7 dB.

this region must receive an adequate explanation; and also the quenching observed at values of magnetic field differing materially from this specific value. The explanation of this axial-mode interaction seems a more difficult problem, since normally such mode interaction between the circularly polarized components is less than the interaction between the circularly polarized oscillations derived from the splitting of a single axial mode in near-zero magnetic fields.

We proceed first by making a few general comments on such mode interactions in lasers in the presence of axial magnetic fields. For clarity we refer to the particular $J=1 \rightarrow 0$ transition applicable to the present investigations, but the remarks are perfectly general and apply to all laser transitions in any axial magnetic field. Assuming such a field for simplicity considering a short laser so that only one axial mode operates on each Zeeman component, it is clear that only two laser oscillations of opposite circular polarizations will occur, in general, for any value of magnetic field, and for any J value of the upper and lower states of the transition. The interaction between these oscillations is still governed by equations of the type

$$\begin{aligned}\dot{E}_1 &= \alpha_1 E_1 - \beta_1 E_1^3 - \theta_{12} E_2^2 E_1, \\ \dot{E}_2 &= \alpha_2 E_2 - \beta_2 E_2^3 - \theta_{21} E_1^2 E_2,\end{aligned}\quad (1)$$

first used by Lamb in his discussion of the interaction between axial modes of the laser within a single Doppler-broadened transition.⁸ In the present case, the coupling is due to the common lower state of the transition, and to the natural linewidths of the upper and lower states of the transition. In particular, resonances may be expected when the Zeeman separation between the $m=\pm 1$ states is close to the axial-mode separation of the laser, which will lead to a strong interaction in this region. The coefficients in Eqs. (1) are functions of the cavity tuning, atomic lifetimes, pressure, magnetic field, Doppler parameter Ku , and the J values of the atomic levels concerned in the laser emission. As already noted, the detailed behavior of various atomic transitions will vary though the general features of the interaction will persist.

An examination of the stability of the singular points of Eqs. (1)¹² shows that simultaneous oscillations of opposite circular polarizations will occur when $\beta_1\beta_2 > \theta_{21}\theta_{12}$. One oscillation, (say E_1), will quench the other (E_2) when $\theta_{21}\alpha_1 > \alpha_2\beta_1$, and, similarly with subscripts 1 and 2 interchanged. It is necessary, of course, that the condition $\beta_1\beta_2 > \theta_{21}\theta_{12}$ be satisfied before such quenching occurs. When $\beta_1\beta_2 < \theta_{21}\theta_{12}$, corresponding to a saddle point, the occurrence of simultaneous oscillations on both polarizations no longer represents a stable situation, and which steady-state single oscillation is reached depends on the initial conditions. When $\beta_1\beta_2 = \theta_{21}\theta_{12}$, so-called neutral coupling, the

situation is rather critically dependent on slight perturbations of the system and may go either way, to a saddle point or to stable two-frequency operation.

If stable two-frequency oscillations occur, their frequencies are determined by the equations

$$\begin{aligned}\nu_1 &= \Omega_1 + \sigma_1 - \rho_1 E_1^2 - \tau_{12} E_2^2, \\ \nu_2 &= \Omega_2 + \sigma_2 - \rho_2 E_2^2 - \tau_{21} E_1^2,\end{aligned}\quad (2)$$

where the coefficients are again functions of all the parameters listed above, and Ω represents an eigenfrequency of the lossless cavity. In near-zero magnetic field where $\Omega_1 = \Omega_2$, these frequencies may become identical because of a relative balance between frequency pulling and pushing effects. This certainly will occur in near-zero magnetic fields as the cavity tunes through line center. If both oscillations occur in such regions, they may lock on a common frequency and give linear or elliptical polarization, and a rotation of the polarization with magnetic field. In such a case, the cavity anisotropy will play a dominant role in determining the component polarizations, particularly in near-zero magnetic fields. Another possibility, particularly if the point of operation in zero magnetic field tends to be a saddle point, is that one of the oscillations (the stronger one at the particular position and direction of cavity tuning) may have quenched the other and captured it, this oscillation then persisting as the cavity is turned through line center in that particular direction, and vice versa for the other oscillation when the cavity is tuned in the opposite direction. Such a possibility would explain the quenching and hysteresis encountered in the present experiments and by others.^{6,7}

Such frequency-locking effects cannot occur when distinct axial modes of the laser operate on well resolved Zeeman components. Here the condition $\beta_1\beta_2 > \theta_{21}\theta_{12}$ is usually satisfied even when the Zeeman separation equals the cavity-mode spacing, and the two axial modes are symmetrical with respect to the Zeeman components. However, for deviations of the magnetic field from this value, and the cavity detuned from this position, it is possible for the condition $\theta_{12}\alpha_2 > \alpha_1\beta_2$ to be satisfied and mode 2 will then quench mode 1, while for the opposite direction of cavity tuning mode 1 will quench mode 2. Such a process would explain the crossover regions near the symmetrical tuning position where both modes oscillate, and also the quenching effects on either side of this region.

Since the interaction between the circularly polarized oscillations on separate axial modes is less than that between such oscillations on one axial mode, one of the main problems will be to modify the theory and to adjust the parameters and atomic linewidths so that the appropriate variation of the coefficients in Eqs. (1) may be obtained and agreement found with the experimental observations.

¹² W. Culshaw and J. Kannelaud, Phys. Rev. **145**, 257 (1966).

IV. THEORY OF THE INTERACTION

The effect of an axial magnetic field on a $J=1 \rightarrow 0$ laser transition may be considered by extending Lamb's theory of the optical maser⁸ to include the vector polarization of the field, and the different transitions involved.^{12,13} For the present work we shall follow the method described in Ref. 12. Figure 9 shows the various quantities involved, and we require the values of the off-diagonal components ρ_{ad} and ρ_{cd} of the density matrix to third order in the perturbations E_1 and E_2 , which correspond to laser emissions in right- and left-handed circular polarizations, respectively. The first-order contribution to the atomic polarization terms may be written down immediately as

$$P_{ad}^{(1)}(t) = -C_1 \bar{N} E_2 e^{-i(\nu_2 t + \phi_2)} Z(\nu_2 - \omega_2) + \text{c.c.} \quad (3)$$

Here \bar{N} is the excitation given by

$$\bar{N} = (1/L) \int_0^L N(z,t) dz, \quad \text{and} \quad C_1 = \frac{1}{2} |\Delta_2|^2 / (\hbar K u), \quad (4)$$

where $N(z,t)$ is the excitation density, which is assumed the same for all similar Fourier projections onto the cavity mode. Z is the plasma dispersion function, which we write as

$$Z(\zeta) = 2i \int_0^\infty e^{-(x^2 - 2\eta x + 2i\xi x)} dx, \quad (5)$$

where

$$x = \frac{1}{2} K u \tau, \quad \zeta = \xi + i\eta, \quad \eta = \gamma_{ad} / (K u), \\ \xi_i = (\nu_1 - \omega_i) / (K u), \quad \gamma_{ad} = \frac{1}{2} (\gamma_a + \gamma_d).$$

Here ω_i and ν_i are the atomic and laser frequencies, respectively, and $K u$ is the Doppler parameter. The equation for $P_{cd}^{(1)}(t)$ is obtained by interchange of subscripts 1 and 2. We note that the Z function depends on the ratio $\gamma_{ad} / K u$, and that Eq. (3) remains valid for all values of this ratio.

The third-order contributions to P_{ad} and P_{cd} are determined by using the iteration procedure and summing the various contributions.^{8,12} In the calculations of the Fourier projection of, say, $P_{ad}^{(3)}(t)$ onto the n th cavity mode integrals of the form

$$(2/L) \int_0^L N(z,t) U_n(z) U_\mu(z - v\tau') U_\rho(z - v\tau' - v\tau'') \\ \times U_\sigma(z - v\tau' - v\tau'' - v\tau''') \quad (6)$$

appear, where

$$U_n(z) = \sin K_n z; \quad K_n = n\pi/L. \quad (7)$$

Retaining only slowly varying terms, and the even functions, the product of the four sine functions can be reduced to

$$\frac{1}{8} \cos K_\alpha z \cos K v(\tau' - \tau''') + \cos K_\beta z \cos K v(\tau''' + \tau') \\ + \cos K_\gamma z \cos K v(\tau' + 2\tau'' + \tau'''), \quad (8)$$

¹³ R. L. Fork and M. Sargent, III, Phys. Rev. **139**, A617 (1965).

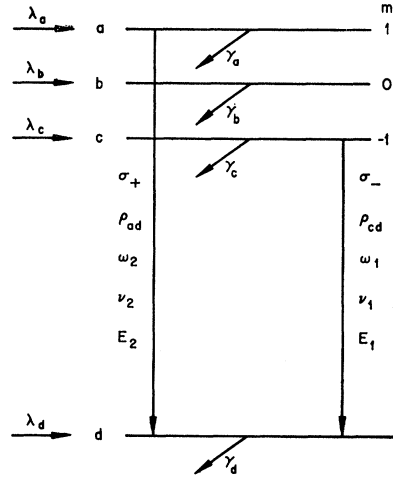


FIG. 9. Transitions and parameters used to consider laser-mode interaction in an axial magnetic field.

where

$$K_a = K_\rho - K_\sigma + K_\mu - K_n, \\ K_b = K_\rho - K_\sigma - K_\mu + K_n, \\ K_c = K_\rho + K_\sigma - K_\mu - K_n. \quad (9)$$

The contributions from the terms in Eq. (8) are examined in detail later. Usually only the first term is retained, and the integration in Eq. (6) is carried out, together with the integration over an assumed Maxwellian velocity distribution. For a single axial mode acting on the Zeeman components in near-zero magnetic fields, we have $\mu = \rho = \sigma = n$, and Eq. (6) reduces to the expression for \bar{N} given by Eq. (4). This factor thus occurs in the terms involved in the third-order expressions for the atomic polarizations. This is not the case when two axial modes act on well-resolved Zeeman components, and in general a term of the form

$$N_{2(n-\mu)}(t) = \frac{1}{L} \int_0^L N(z,t) \cos 2(n-\mu) \frac{\pi z}{L} dz \quad (10)$$

occurs, representing a spatial Fourier component of the excitation density. For two adjacent axial modes, $n - \mu = 1$, although the results remain valid for any two axial modes of the laser cavity. The factor N_2 is dependent on the function $N(z,t)$, but will usually be negative, and this leads to the result that the interaction between Zeeman-component oscillations on the two separate axial modes is less than that between such oscillations derived from a single axial mode.

Proceeding as in Ref. 12, and using the delta-function approximation⁸ in the third-order integrals of the type

$$\int_0^\infty d\tau' \int_0^\infty d\tau'' \int_0^\infty d\tau''' e^{-[\gamma_{ad} + i(\omega_i - \nu_i)]\tau'} e^{\gamma_a \tau''} \\ \times e^{-[\gamma_{ad} + i(\omega_j - \nu_j)]\tau'''} e^{-\frac{1}{2}(K u)^2 (\tau' - \tau''')^2}, \quad (11)$$

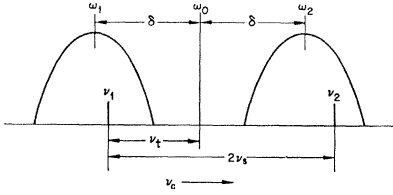


FIG. 10. Tuning parameters used to consider axial-mode interaction in a Zeeman laser.

we obtain

$$\begin{aligned}
 P_{ad}^{(3)}(t) = & iC_2 \bar{N} E_2^3 e^{-(\nu_2 t + \phi_2)} 2\pi^{1/2} \\
 & \times \{ \gamma_{ad} [\gamma_{ad} + i(\omega_2 - \nu_2)]^{-1} + 1 \} + iC_2 \bar{N} E_1^2 E_2 e^{-i(\nu_2 t + \phi_2)} \\
 & \times \pi^{1/2} \{ \gamma_a [\gamma_{ad} + i(\omega_{21} - \nu_{21})]^{-1} + (\gamma_{ad} + i\delta_{21})^{-1} \} \\
 & + \gamma_a \gamma_d (\gamma_{ad} + i\delta_{21})^{-1} (\gamma_a + i2\delta_{21})^{-1} + (N_2/\bar{N}) \gamma_a \gamma_d \\
 & \times [\gamma_{ad} + i(\omega_2 - \nu_2)]^{-1} (\gamma_a + i2\delta_{21})^{-1} \} + \text{c.c.}, \quad (12)
 \end{aligned}$$

with the equation for $P_{cd}^{(3)}(t)$ obtained by interchanging the subscripts 1 and 2, and where

$$\begin{aligned}
 C_2 = & |\Delta_2|^4 / (32\hbar^3 K \omega \gamma_a \gamma_d), \\
 \delta_{mn} = & \frac{1}{2} [\omega_m - \omega_n - (\nu_m - \nu_n)], \\
 \omega_{mn} = & \frac{1}{2} (\omega_m + \omega_n), \\
 \nu_{mn} = & \frac{1}{2} (\nu_m + \nu_n); \quad m, n = 1, 2.
 \end{aligned} \quad (13)$$

We shall have reason to examine closely the delta-function approximation used to evaluate Eq. (11). This implies the condition $Ku \gg \gamma_{ad}$, but the approximation is not really valid for any value of Ku , although it is a good one for the condition states and for not too wide deviations of cavity tuning from line center. The difference between the mode interactions in small and in large magnetic fields is shown by the factor N_2/\bar{N} , which becomes +1 in the former case, and which for the interaction between axial modes is negative, possibly around -0.5, depending on the excitation density $N(z, t)$.

The interaction coefficients in the nonlinear Eqs. (1) and (2) are now obtained by substituting the atomic polarization terms given by Eqs. (3) and (12) into the conditional equation

$$\begin{aligned}
 \frac{1}{2} \mathbf{e} \{ -i(2\nu_n \dot{E}_n + \nu \nu_n E_n / Q_n) + E_n 2\Omega_n \\
 \times [\Omega_n - (\nu_n + \phi_n)] \} e^{-i(\nu_n t + \phi_n)} + \text{c.c.} \\
 = \frac{1}{2} \mathbf{e} (\nu^2 / \epsilon_0) P_n(t) e^{-i(\nu_n t + \phi_n)} + \text{c.c.}, \quad (14)
 \end{aligned}$$

and equating the real and imaginary parts. Here the unit vector \mathbf{e} represents the polarization of the emitted radiation. Since we shall be specifically interested in the variation of the interaction between axial modes with cavity tuning and magnetic field, we recast these equations as follows. Referring to Fig. 10, where ν_i represents the deviation of the frequency ν_1 from line center and $2\nu_s$ represents the axial-mode separation,

we deduce that

$$\begin{aligned}
 \omega_2 - \nu_2 = & -(P + T), \\
 \omega_1 - \nu_1 = & P - T, \\
 \omega_{21} - \nu_{21} = & -T, \\
 \delta_{21} = & -P,
 \end{aligned} \quad (15)$$

where $T = \nu_s - \nu_i$ represents the deviation of cavity tuning from the symmetrical position, and $P = \nu_s - \delta$, where $\delta = \gamma H$ ($\gamma =$ gyromagnetic ratio) represents the deviation of the Zeeman separation from the axial-mode separation. In this way we obtain the results

$$\begin{aligned}
 \alpha_2 = & C_1 [Z_i(A) - \eta_i^{-1} Z_i(0)], \\
 \beta_2 = & \text{Im} i C_2 \pi^{1/2} [\gamma_{ad} (\gamma_{ad}' - i(P + T))^{-1} + 1], \\
 \theta_{21} = & \text{Im} i C_2 \pi^{1/2} \{ \gamma_a [(\gamma_{ad}' - iT)^{-1} + (\gamma_a - iP)^{-1}] \\
 & + \gamma_a \gamma_d (\gamma_a - i2P)^{-1} \\
 & \times [(\gamma_{ad} - iP)^{-1} + N_d (\gamma_{ad}' - i(P + T))^{-1}] \}, \quad (16)
 \end{aligned}$$

where

$$A = (P + T) / Ku,$$

with similar equations for α_1 , $\beta_{1,1}$ and θ_{12} obtained by changing the sign of P . Here $N_d \equiv N_2/\bar{N}$ takes the value +1 for a single axial mode, and becomes negative, as above, for axial-mode interaction. The coefficients σ , ρ , and τ in the frequency equations are given by the real part of these expressions and of the Z function. We have also inserted a factor γ_{ad}' in all terms involving the interaction of the cavity radiation with the atomic transition, after the work of Szöke and Javan on the effect of atomic collisions.

Under the approximations made, Eqs. (16) represent the interaction both in near-zero fields and between distinct axial modes operating on well-resolved Zeeman components. They should show the variation in the intensities of the coupled oscillations as a function of T and P . Curves may be deduced as a function of cavity tuning for fixed values of P . For interaction between two axial modes, positive values of P correspond to Zeeman separations less than the axial-mode interval, and the maximum value of β_2 , say, occurs at $T = -P$. Similar results hold for the other parameters, and the maximum of the $\Delta m = +1$ transition will occur on opposite sides of the line center as P changes sign and the cavity is tuned over the linewidth. This conclusion agrees with the experimental results shown in Fig. 4. Further investigation of Eqs. (16) shows that $\beta_1 \beta_2 = \theta_{12} \theta_{21}$ in zero magnetic field, and hence a saddle-point tendency exists. The quenching effects in near-zero magnetic fields may also be explained by adjusting the atomic parameters, and analogous equations have been used by Fork and Tomlinson¹⁴ in similar work on the $J=1 \rightarrow 0$ He-Ne transition at 1.52 μ . It becomes apparent, however, that the strong axial-mode inter-

¹⁴R. L. Fork and W. J. Tomlinson, Paper 4A-9, in Fourth International Quantum Electronics Conference, Phoenix, Arizona, 1966 (unpublished), and private communication.

actions, including quenching effects such as observed in xenon, cannot be adequately explained by these equations, and a more accurate treatment of the third order polarization terms is required.

V. APPLICATION TO THE Xe TRANSITION

The parameter Ku for Xe is around 100 Mc/sec for an assumed atomic temperature of 515°K, and the exact integration of Eq. (11) and similar third-order contributions is necessary. This may be done using the result¹⁵

$$\int_0^\infty \int_0^\infty dx dy e^{2i(\xi_a x + \xi_b y) - 2\eta(x+y) - (x-y)^2} = (8i\eta)^{-1} (1 - i\xi/\eta)^{-1} [Z(\xi_a) + Z(\xi_b)], \quad (17)$$

which may be verified by the substitutions $\alpha = x - y$,

$$\int_0^\infty \int_0^\infty e^{-4(\eta\alpha z - z^2)} dz \int_0^\infty \int_0^\infty e^{2i(\xi_a x + \xi_b y) - 2(\eta+2z)(x+y) - (x+y)^2} dx dy = -\frac{1}{4} \int_0^\infty e^{-4(\eta\alpha z - z^2)} \frac{Z(\xi_a, \eta+2z) - Z(\xi_b, \eta+2z)}{\xi_a - \xi_b} dz. \quad (19)$$

Here the term in the integral involving a difference of Z functions is slowly varying with z as compared to the exponential term, and we approximate the z integral by the expression

$$-\frac{1}{16i} Z(0, \eta_a) \frac{Z(\xi_a, \eta) - Z(\xi_b, \eta)}{\xi_a - \xi_b}, \quad (20)$$

where $\eta_a = \gamma_a / (2Ku)$, and $z = \frac{1}{2} Ku \tau''$.

Using Eqs. (17), (18), and (20), together with the results of Ref. 12, the following more exact equations are obtained for the interaction parameters in an axial magnetic field:

$$\beta_2 = \text{Im} \{ (Ku \gamma_a \gamma_d)^{-1} [2\gamma_{ad}(\gamma_{ad}' - i(P+T))^{-1} Z(A) + 2Z_i(A)] - [i2\gamma_{ad}/\gamma_a \gamma_d (Ku)^2] [Z'(A) + Z_r(A)/A] - \frac{1}{2} (Ku)^{-3} [Z(0, \eta_a) + Z(0, \eta_d)] [Z'(A) + Z_r(A)/A] \}, \quad (21)$$

where the three terms in inverse powers of Ku correspond to the three contributions obtained using Eqs. (17), (18), and (19), and $\eta_d = \gamma_d / (2Ku)$. The constant $C_2 \bar{N} \gamma_a \gamma_d Ku$ is omitted in Eq. (21). Similarly, we find

$$\begin{aligned} \theta_{21} = & \text{Im} \{ 2\gamma_d Ku^{-1} [(\gamma_{ad}' - iT)^{-1} (Z(A) + Z(-B)) + (\gamma_{ad} - iP)^{-1} (Z(A) + Z(B))] + (2Ku)^{-1} (\gamma_a - i2P)^{-1} \\ & \times [(\gamma_{ad} - iP)^{-1} (Z(A) + Z(B)) + 2N_d (\gamma_{ad}' - i(P+T))^{-1} Z(A) - \frac{i}{\gamma_d (Ku)^2} \left[\frac{Z(A) - Z(-B)}{2P/(Ku)} + \frac{Z(A) - Z(B)}{2T/(Ku)} \right] \right. \\ & \left. + \gamma_d (\gamma_a - i2P)^{-1} \left(Z'(A) + N_d \frac{Z(A) - Z(B)}{2T/(Ku)} \right) \right] - \frac{1}{2} (Ku)^{-3} \left[N_d Z(0, \eta_d) \left(\frac{Z(A) - Z(-B)}{2P/(Ku)} + \frac{Z(A) - Z(B)}{2T/(Ku)} \right) \right. \\ & \left. + Z(P/(Ku), \eta_a) \left(Z'(A) + \frac{Z(A) - Z(B)}{2T/(Ku)} \right) \right] \}, \quad (22) \end{aligned}$$

where Z' represents the derivative with respect to the real part of the argument, and $B = (P - T)/(Ku)$. The coefficients β_1 and θ_{12} follow from Eqs. (21) and (22) by changing the sign of P , and the frequency parameters ρ and τ are given by the real parts of these expressions. Comparing Eqs. (16) and (21), we see that the first-order or delta-function approximation is reasonable only for

¹⁵ F. Aronowitz, Phys. Rev. **139**, A635 (1965).

$\beta = x + y$. Here $y = \frac{1}{2} Ku \tau'''$, $\xi_i = (\nu_i - \omega_i)/Ku$, and $\xi = \frac{1}{2}(\xi_a + \xi_b)$, with x and η as defined previously. This term, derived from that involving $\cos K\tau(\tau' - \tau''')$ in Eq. (8), gives the main contribution to the third-order atomic polarization. However, the other terms, involving $(\tau' + \tau''')$ and $(\tau' + 2\tau'' + \tau''')$, in Eq. (8) are not negligible in the case of Xe, since the atomic linewidths are comparable with Ku .¹⁶ The first of these may be considered using the integral¹⁵

$$\int_0^\infty \int_0^\infty dx dy e^{2i(\xi_a x + \xi_b y) - 2\eta(x+y) - (x+y)^2} = -\frac{1}{4} [Z(\xi_a) - Z(\xi_b)] / (\xi_a - \xi_b). \quad (18)$$

The contribution to Eq. (11) from the term in $(\tau' + 2\tau'' + \tau''')$

may also be reduced to the form

$$\int_0^\infty \int_0^\infty e^{-4(\eta\alpha z - z^2)} dz \int_0^\infty \int_0^\infty e^{2i(\xi_a x + \xi_b y) - 2(\eta+2z)(x+y) - (x+y)^2} dx dy = -\frac{1}{4} \int_0^\infty e^{-4(\eta\alpha z - z^2)} \frac{Z(\xi_a, \eta+2z) - Z(\xi_b, \eta+2z)}{\xi_a - \xi_b} dz. \quad (19)$$

Here the term in the integral involving a difference of Z functions is slowly varying with z as compared to the exponential term, and we approximate the z integral by the expression

$$-\frac{1}{16i} Z(0, \eta_a) \frac{Z(\xi_a, \eta) - Z(\xi_b, \eta)}{\xi_a - \xi_b}, \quad (20)$$

where $\eta_a = \gamma_a / (2Ku)$, and $z = \frac{1}{2} Ku \tau''$.

Using Eqs. (17), (18), and (20), together with the results of Ref. 12, the following more exact equations are obtained for the interaction parameters in an axial magnetic field:

$$\beta_2 = \text{Im} \{ (Ku \gamma_a \gamma_d)^{-1} [2\gamma_{ad}(\gamma_{ad}' - i(P+T))^{-1} Z(A) + 2Z_i(A)] - [i2\gamma_{ad}/\gamma_a \gamma_d (Ku)^2] [Z'(A) + Z_r(A)/A] - \frac{1}{2} (Ku)^{-3} [Z(0, \eta_a) + Z(0, \eta_d)] [Z'(A) + Z_r(A)/A] \}, \quad (21)$$

where the three terms in inverse powers of Ku correspond to the three contributions obtained using Eqs. (17), (18), and (19), and $\eta_d = \gamma_d / (2Ku)$. The constant $C_2 \bar{N} \gamma_a \gamma_d Ku$ is omitted in Eq. (21). Similarly, we find

$$\begin{aligned} \theta_{21} = & \text{Im} \{ 2\gamma_d Ku^{-1} [(\gamma_{ad}' - iT)^{-1} (Z(A) + Z(-B)) + (\gamma_{ad} - iP)^{-1} (Z(A) + Z(B))] + (2Ku)^{-1} (\gamma_a - i2P)^{-1} \\ & \times [(\gamma_{ad} - iP)^{-1} (Z(A) + Z(B)) + 2N_d (\gamma_{ad}' - i(P+T))^{-1} Z(A) - \frac{i}{\gamma_d (Ku)^2} \left[\frac{Z(A) - Z(-B)}{2P/(Ku)} + \frac{Z(A) - Z(B)}{2T/(Ku)} \right] \right. \\ & \left. + \gamma_d (\gamma_a - i2P)^{-1} \left(Z'(A) + N_d \frac{Z(A) - Z(B)}{2T/(Ku)} \right) \right] - \frac{1}{2} (Ku)^{-3} \left[N_d Z(0, \eta_d) \left(\frac{Z(A) - Z(-B)}{2P/(Ku)} + \frac{Z(A) - Z(B)}{2T/(Ku)} \right) \right. \\ & \left. + Z(P/(Ku), \eta_a) \left(Z'(A) + \frac{Z(A) - Z(B)}{2T/(Ku)} \right) \right] \}, \quad (22) \end{aligned}$$

$Ku \gg \gamma_{ad}$, and for ranges of cavity tuning and magnetic field which are small compared with Ku . Significant changes occur as the imaginary part of the Z function starts to decrease, and as the real part increases with the arguments. In particular, the β_2 coefficient no longer approaches an asymptotic value but steadily

¹⁶ We are indebted to J. Winocur for helpful discussion and emphasis on this point.

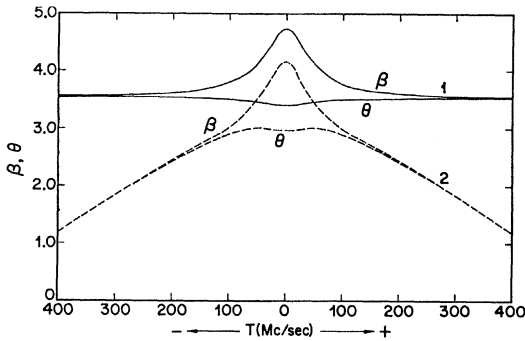


FIG. 11. Variation of parameters β and θ with cavity tuning for $P=0$. Curves No. 1, δ -function approximation to third-order integrals. Curves No. 2, exact integration of third-order terms. $Ku=384$, $\gamma_{ad}'=48$, $\gamma_{ad}=16$, $\gamma_a=24$, $\gamma_a=8$, all expressed in Mc/sec. $N_d=-0.5$.

decreases with cavity tuning. These and other differences in the behavior of the coefficients are of particular significance in the explanation of the strong interaction between axial modes of a laser. Figure 11 shows the saturation coefficient β and interaction coefficient θ as a function of cavity tuning T for $P=0$. Curves are shown for the δ -function approximation, and for the more exact integration with $Ku=384$ Mc/sec and $\gamma_{ad}'=48$ Mc/sec, etc. as indicated.

The terms in increasing inverse powers of Ku in Eq. (21) for β_2 are shown in Fig. 12, together with their

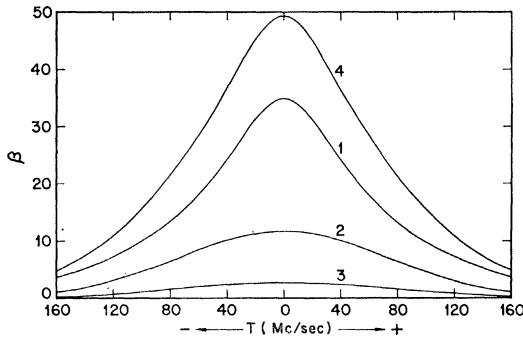


FIG. 12. Contributions to saturation parameter β versus cavity tuning for $P=0$. Curve No. 1, main term from $\tau'-\tau'''$; curve No. 2, contribution from $\tau'+\tau'''$; curve No. 3, contribution from $\tau'+2\tau''+\tau'''$. Curve No. 4, sum of contributions $Ku=96$, $\gamma_{ad}'=48$, $\gamma_{ad}=32$, $\gamma_a=40$, $\gamma_a=24$, expressed in Mc/sec.

summation. These were deduced for the values $Ku=96$, $\gamma_{ad}'=48$, $\gamma_{ad}=32$, $\gamma_a=40$, and $\gamma_a=24$, expressed in Mc/sec. It is seen that the contribution from the term involving $(\tau'+2\tau''+\tau''')$ is small which implies that no serious error should result from the approximation used in the integration of Eq. (19). The contribution from the term in $(Ku)^{-2}$ is significant for the above parameters, and the relative magnitude of the terms changes with P and T . Figure 13 shows the similar contributions to θ_{21} for these parameters and again for $P=0$, the main contributions being due to the terms involving $\tau'-\tau'''$ and $\tau'+\tau''$ in Eq. (8). These curves

apply to oscillations on different axial modes, and the parameter N_d in Eq. (22) is taken as -0.5 . For $N_d=+1$, corresponding to similar oscillations derived from the frequency splitting of a single axial mode in small magnetic fields, the coefficient θ_{21} for $P=0$ becomes the same as the coefficient β_2 shown in Fig. 12, with similar results for β_1 and θ_{12} , which are all equal in this case. This again indicates neutral coupling in near-zero magnetic fields, as indicated earlier. Finally, Fig. 14 shows the variation in the intensities of the coupled oscillations on adjacent axial modes with cavity tuning for various values of P . For $P=0$, or the Zeeman separation of the $m=\pm 1$ levels equal to the axial-mode separation, the intensities of the two oppositely cir-

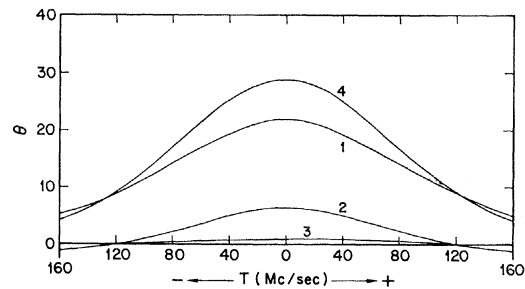


FIG. 13. Contributions to interaction parameter θ versus cavity tuning for $P=0$. Curve No. 1, main term from $\tau'-\tau'''$; curve No. 3, contribution from $\tau'+2\tau''+\tau'''$. Curve No. 4, sum of contributions. $Ku=96$, $\gamma_{ad}'=48$, $\gamma_{ad}=32$, $\gamma_a=40$, $\gamma_a=24$, expressed in Mc/sec.

cularly polarized oscillations are equal for all positions of cavity tuning. For finite values of P crossovers in the intensities and quenching effects occur, as shown by the curves for $P=8$ and 50 Mc/sec.

The shape of the curves changes with the parameters used and with the relative excitation η_t , but the general features of the interaction persist.

VI. CONCLUSIONS

We have not attempted to fit any of the experimental curves at this time, but have been concerned with the

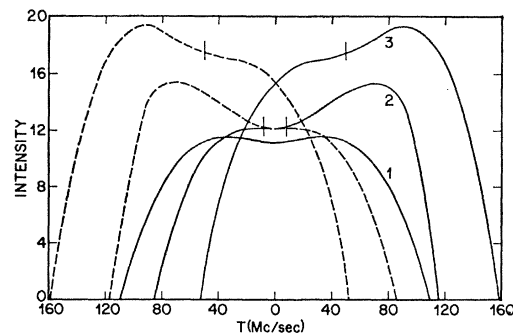


FIG. 14. Intensities of adjacent axial modes oscillating on well-resolved Zeeman components versus cavity tuning. Full curves $m=-1 \rightarrow 0$ transition; dashed curves $m=1 \rightarrow 0$ transition. Curves No. 1, 2, and 3 for $P=0, 8$, and 50 Mc/sec, respectively. $Ku=96$, $\gamma_{ad}'=48$, $\gamma_{ad}=32$, $\gamma_a=40$, $\gamma_a=24$, $\eta_t=2$.

qualitative explanation of the observed mode interactions on the basis of Lamb's theory.⁸ The empirical variation of the parameters, particularly of the lifetimes and atomic response, can produce quenching in near-zero fields even in the first-order approximation, which is reasonably valid for $Ku \gg \gamma_{ad}$, and for tuning positions near line center. However, any explanation of the axial-mode interactions, particularly in xenon, requires the more accurate expressions for the interaction and saturation coefficients derived here. In any event, they are required when large ranges of cavity tuning are involved.

Comparing the curves in Fig. 14 with the experimental results shown in Fig. 4, it is apparent that the quantitative agreement is not particularly good. The quenching is not as sharp as is observed over a range of levels of excitation, and the effects due to the Lamb dip persist in the theoretical results for the parameters used here. In addition, the level of intensity at the crossover when $T=0$ varies with magnetic field in the curves of Fig. 14, which is not apparent in the experimental curves. This prediction leads to dips in the intensities of the modes as the magnetic field is scanned for various values T of cavity tuning, in contrast to the experimental results shown in Fig. 7. It is possible that the 14% isotopic content of Xe^{134} affects the experimental results in this region, and further investigations are necessary using a purer isotope. The effects of collisions on the phenomena are also not known too well at present. Questions regarding relaxation between the Zeeman sublevels due to collisions and changes in the alignment and orientation of the excited state may also be

significant.¹⁷ Such changes can be ascribed to a change in the lifetime of the excited state, which could be introduced into the equations in an empirical way to give better agreement. Further investigations are, however, required to substantiate any such procedure.

The situation in near-zero magnetic fields with a $J=1 \rightarrow 0$ laser transition is largely dependent on the history and operating conditions because of the presence of neutral coupling, which the theory predicts. Any slight perturbation in the reflectors, cavity alignment, intensity, excitation densities (which we have assumed equal for all Zeeman transitions), pressure, etc., has a large effect on the character of the laser emission in this region. The application of a magnetic field reduces this erratic behavior somewhat, though nonlinear effects, such as frequency locking or the capture of the weaker oscillation by the stronger one, are still possible in regions of near-zero beat frequency. Such effects most likely play a dominant role in the observed hysteresis effects in near-zero magnetic fields, though we have not considered such complicated nonlinear phenomena in any detail.

ACKNOWLEDGMENTS

We express our thanks to B. L. Fowles for the construction and operation of the short planar laser, and for instrumentation and assistance throughout the experiments. We also thank M. Stewart for assistance and for programming the numerical computations.

¹⁷ W. Hopper and E. B. Soloman, Phys. Rev. Letters **15**, 441 (1965).